

Supplementary: Structure-Aware Motion Deblurring Using Multi-Adversarial Optimized CycleGAN

Yang Wen, Jie Chen, Bin Sheng, *Member, IEEE*, Zhihua Chen, Ping Li, *Member, IEEE*,
Ping Tan, *Senior Member, IEEE*, and Tong-Yee Lee, *Senior Member, IEEE*

Abstract—This supplementary document provides more experimental results together with the ground truth images, which could not be fit in the main paper due to the page limit.

I. ABLATION STUDY

A. Comparison on Multi-Adversarial Architecture

Fig. 1 shows some results of multi-adversarial architecture G_S with three different discriminators. Fig. 1(b) is the result at the final resolution level (256×256) with single discriminator D_{S256} . Fig. 1(c) and Fig. 1(d) are the results at the final resolution level (256×256) with two discriminators D_{S128} and D_{S256} and with three discriminators D_{S64} , D_{S128} and D_{S256} , respectively. It illustrates that deblurring effects can be improved with the increase of adversarial constraint level.

B. Comparison on Different Unsupervised and Supervised CNN-Based Methods

Fig. 2 shows the deblurring results by different methods. Compared with other classical methods, especially the supervised CNN-based method [2] and unsupervised GAN-based method [1], our method has obvious advantages for motion deblurring. It also shows the effectiveness of our multi-adversarial learning architecture.

C. Comparison on Different Components in Our Model

Fig 3 shows the visual effectiveness of different components in our model. Fig 3(a) are the results by the original CycleGAN (as baseline). Fig 3(b) are the results by the baseline with multi-adversarial loss. Fig 3(c) are the results by item

Manuscript received December 12, 2020; revised May 15, 2021; accepted June 15, 2021. This work was supported in part by the National Natural Science Foundation of China under Grant 61872241 and Grant 61572316, in part by The Hong Kong Polytechnic University under Grant P0030419, Grant P0030929, and Grant P0035358, and in part by the Ministry of Science and Technology, Taiwan under Grant 108-2221-E-006-038-MY3.

Y. Wen and B. Sheng are with the Department of Computer Science and Engineering, Shanghai Jiao Tong University, Shanghai 200240, China (Email: shengbin@sjtu.edu.cn).

J. Chen is with the Samsung Electronics (China) R&D Centre, Nanjing 210012, China (E-mail: ada.chen@samsung.com).

Z. Chen is with the Department of Computer Science and Engineering, East China University of Science and Technology, Shanghai 200237, China.

P. Li is with the Department of Computing, The Hong Kong Polytechnic University, Kowloon, Hong Kong (Email: p.li@polyu.edu.hk).

P. Tan is with the School of Computing Science, Simon Fraser University, Burnaby, BC V5A 1S6, Canada (Email: pingtan@sfsu.ca).

T.-Y. Lee is with the Department of Computer Science and Information Engineering, National Cheng-Kung University, Tainan 70101, Taiwan (Email: tonylee@mail.ncku.edu.tw).

Fig 3(b) with edge input and edge loss. Fig 3 (d) are the results by item Fig 3(c) with MSSIM and perceptual loss. The experimental results show that the key components we proposed in our deblurring model can effectively improve the overall deblurring effect.

II. PERFORMANCE ON BENCHMARK DATASETS

A. Performance Comparison on Text Dataset

Fig. 4 presents several examples from the BMVC_TEXT dataset [3] to illustrate the qualitative comparisons of other methods with ours. In Fig. 4, especially in the central character part, our deblurring results can achieve the clearest characters. These examples are sufficient to prove that our method can achieve quite effective results on BMVC_TEXT dataset [3].

B. Performance Comparison on Real Face Dataset

Fig. 5 presents the visual comparisons with other state-of-the-art approaches on real blurred face images. In Fig. 5, especially in the color border area, the deblurring results by our method can reconstruct more structural information. These examples are sufficient to prove that our method can achieve quite effective results on face dataset [8].

REFERENCES

- [1] J.-Y. Zhu, T. Park, P. Isola, and A. A. Efros, “Unpaired image-to-image translation using cycle-consistent adversarial networks,” in *IEEE International Conference on Computer Vision*, 2017, pp. 2242–2251.
- [2] J. Sun, W. Cao, Z. Xu, and J. Ponce, “Learning a convolutional neural network for non-uniform motion blur removal,” in *IEEE Conference on Computer Vision and Pattern Recognition*, 2015, pp. 769–777.
- [3] M. Hradiš, J. Kotera, P. Zemčík, and F. Šroubek, “Convolutional neural networks for direct text deblurring,” in *British Machine Vision Conference*, 2015, pp. 6:1–6:13.
- [4] J. Pan, Z. Hu, Z. Su, and M.-H. Yang, “Deblurring text images via L_0 -regularized intensity and gradient prior,” in *IEEE Conference on Computer Vision and Pattern Recognition*, 2014, pp. 2901–2908.
- [5] J. Pan, D. Sun, H. Pfister, and M.-H. Yang, “Deblurring images via dark channel prior,” *IEEE Transactions on Pattern Analysis and Machine Intelligence*, vol. 40, no. 10, pp. 2315–2328, 2018.
- [6] L. Xu, S. Zheng, and J. Jia, “Unnatural L_0 sparse representation for natural image deblurring,” in *IEEE Conference on Computer Vision and Pattern Recognition*, 2013, pp. 1107–1114.
- [7] S. Nah, T. H. Kim, and K. M. Lee, “Deep multi-scale convolutional neural network for dynamic scene deblurring,” in *IEEE Conference on Computer Vision and Pattern Recognition*, 2017, pp. 257–265.
- [8] Z. Liu, P. Luo, X. Wang, and X. Tang, “Deep learning face attributes in the wild,” in *IEEE International Conference on Computer Vision*, 2015, pp. 3730–3738.
- [9] T. Kim, M. Cha, H. Kim, J. K. Lee, and J. Kim, “Learning to discover cross-domain relations with generative adversarial networks,” in *International Conference on Machine Learning*, 2017, pp. 1857–1865.

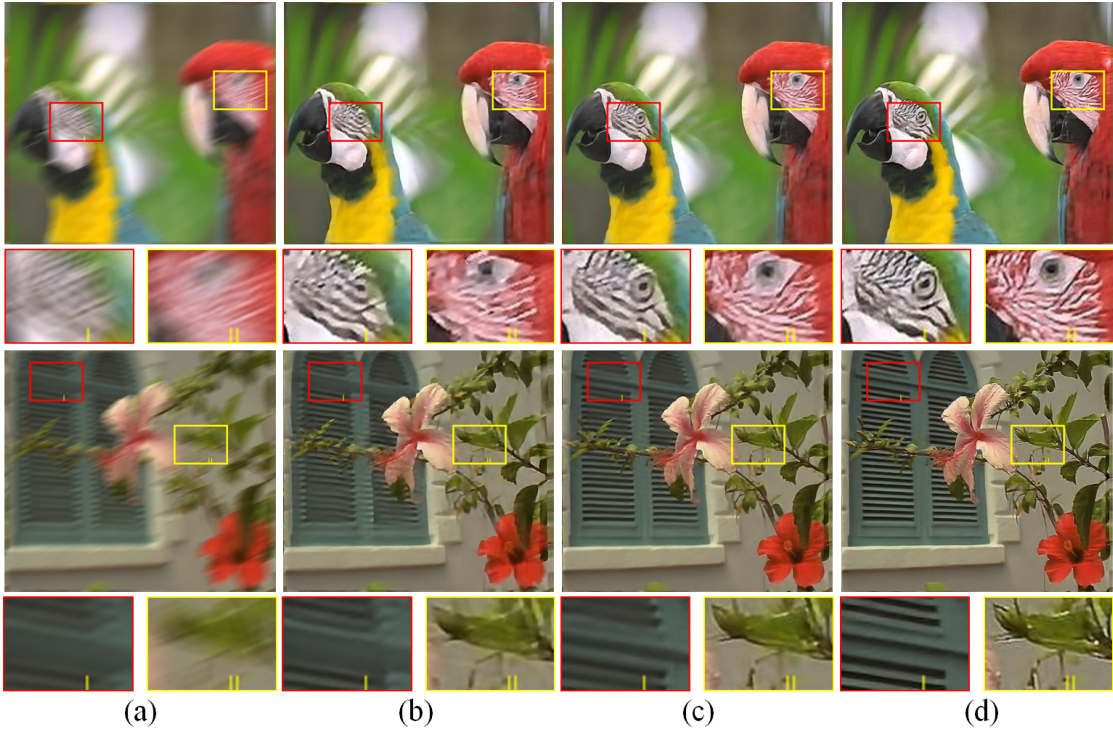


Fig. 1: Deblurred results of multi-adversarial generator. (a) Blurred images. (b) Results with single discriminator D_{S256} . (c) Results with two discriminators D_{S256} and D_{S128} . (d) Results with three discriminators D_{S256} , D_{S128} and D_{S64} .

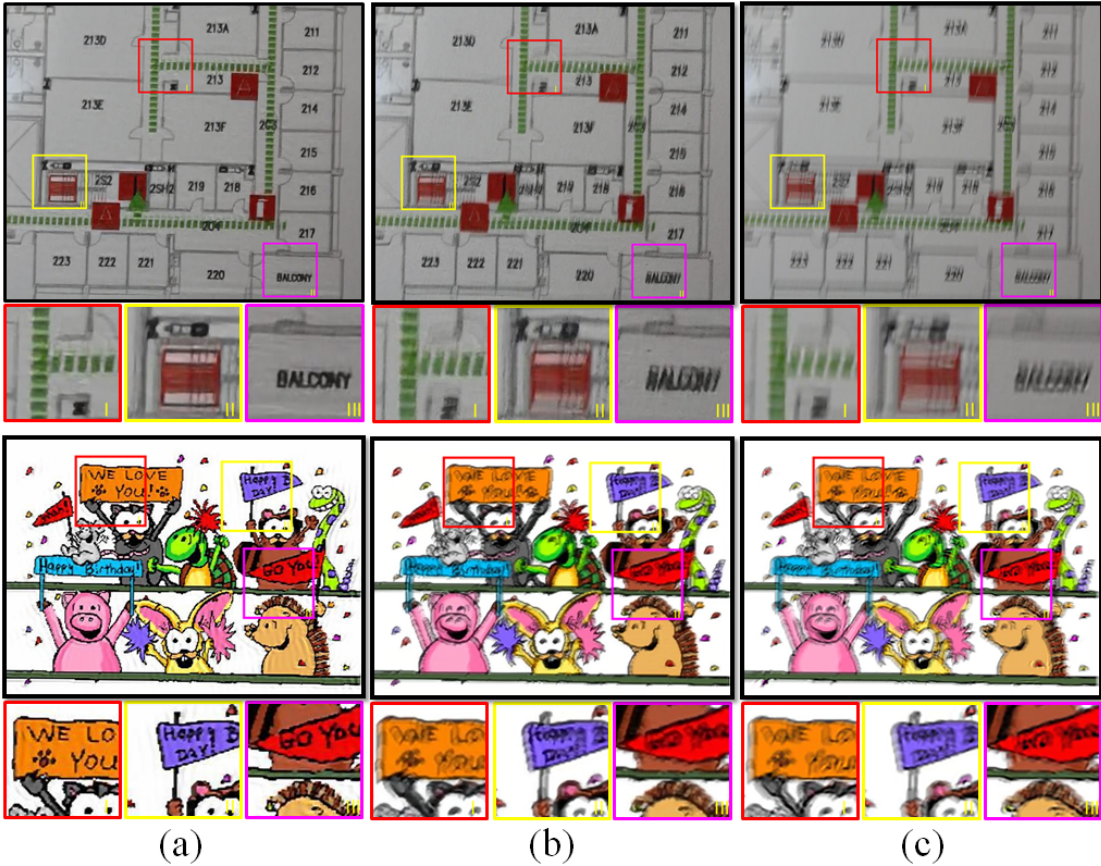


Fig. 2: Comparison of deblurred images by our unsupervised multi-adversarial deblurring method with other classical supervised and unsupervised approaches. (a) Deblurring results by our method. (b) Deblurring results using unsupervised GAN-based method [1]. (c) Deblurring results using supervised CNN-based method Sun *et al.* [2].

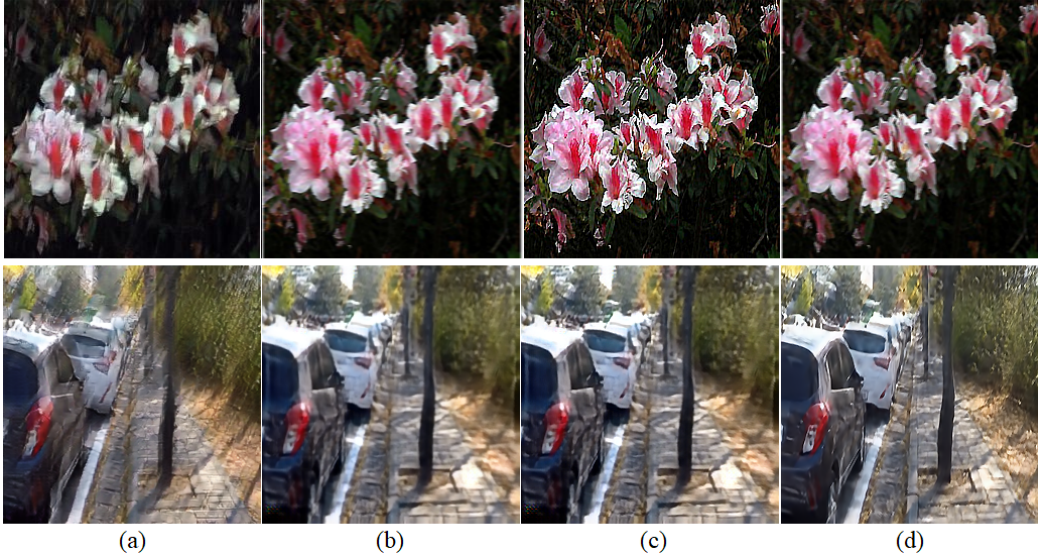


Fig. 3: The visual effectiveness of different components in our model. (a) original CycleGAN (as baseline); (b) baseline + multi-adversarial loss; (c) item (b)+edge input and edge loss; (d) item (c)+MSSIM+perceptual loss. The experimental results show that the key components we proposed can effectively improve the overall deblurring effect.

<small>Gross, L., R. Carley, and T. Kanade. Infrared and range-finding analog signal processor scheme using a camera/laser-sensor. <i>IEEE Transactions on Robotics and Computer-Aided Manufacturing</i>, 12(2):743–750, 1996.</small>	<small>Gross, L., R. Carley, and T. Kanade. Infrared and range-finding analog signal processor scheme using a camera/laser-sensor. <i>IEEE Transactions on Robotics and Computer-Aided Manufacturing</i>, 12(2):743–750, 1996.</small>	<small>Gross, L., R. Carley, and T. Kanade. Infrared and range-finding analog signal processor scheme using a camera/laser-sensor. <i>IEEE Transactions on Robotics and Computer-Aided Manufacturing</i>, 12(2):743–750, 1996.</small>	<small>Gross, L., R. Carley, and T. Kanade. Infrared and range-finding analog signal processor scheme using a camera/laser-sensor. <i>IEEE Transactions on Robotics and Computer-Aided Manufacturing</i>, 12(2):743–750, 1996.</small>	<small>Gross, L., R. Carley, and T. Kanade. Infrared and range-finding analog signal processor scheme using a camera/laser-sensor. <i>IEEE Transactions on Robotics and Computer-Aided Manufacturing</i>, 12(2):743–750, 1996.</small>	<small>Gross, L., R. Carley, and T. Kanade. Infrared and range-finding analog signal processor scheme using a camera/laser-sensor. <i>IEEE Transactions on Robotics and Computer-Aided Manufacturing</i>, 12(2):743–750, 1996.</small>	<small>Gross, L., R. Carley, and T. Kanade. Infrared and range-finding analog signal processor scheme using a camera/laser-sensor. <i>IEEE Transactions on Robotics and Computer-Aided Manufacturing</i>, 12(2):743–750, 1996.</small>
<small>Gross, L., R. Carley, and T. Kanade. Infrared and range-finding analog signal processor scheme using a camera/laser-sensor. <i>IEEE Transactions on Robotics and Computer-Aided Manufacturing</i>, 12(2):743–750, 1996.</small>	<small>Gross, L., R. Carley, and T. Kanade. Infrared and range-finding analog signal processor scheme using a camera/laser-sensor. <i>IEEE Transactions on Robotics and Computer-Aided Manufacturing</i>, 12(2):743–750, 1996.</small>	<small>Gross, L., R. Carley, and T. Kanade. Infrared and range-finding analog signal processor scheme using a camera/laser-sensor. <i>IEEE Transactions on Robotics and Computer-Aided Manufacturing</i>, 12(2):743–750, 1996.</small>	<small>Gross, L., R. Carley, and T. Kanade. Infrared and range-finding analog signal processor scheme using a camera/laser-sensor. <i>IEEE Transactions on Robotics and Computer-Aided Manufacturing</i>, 12(2):743–750, 1996.</small>	<small>Gross, L., R. Carley, and T. Kanade. Infrared and range-finding analog signal processor scheme using a camera/laser-sensor. <i>IEEE Transactions on Robotics and Computer-Aided Manufacturing</i>, 12(2):743–750, 1996.</small>	<small>Gross, L., R. Carley, and T. Kanade. Infrared and range-finding analog signal processor scheme using a camera/laser-sensor. <i>IEEE Transactions on Robotics and Computer-Aided Manufacturing</i>, 12(2):743–750, 1996.</small>	<small>Gross, L., R. Carley, and T. Kanade. Infrared and range-finding analog signal processor scheme using a camera/laser-sensor. <i>IEEE Transactions on Robotics and Computer-Aided Manufacturing</i>, 12(2):743–750, 1996.</small>
<small>Hartley and A. Zisserman. <i>Multiple View Geometry in Computer Vision</i>. Cambridge University Press, 2000.</small>	<small>Hartley and A. Zisserman. <i>Multiple View Geometry in Computer Vision</i>. Cambridge University Press, 2000.</small>	<small>Hartley and A. Zisserman. <i>Multiple View Geometry in Computer Vision</i>. Cambridge University Press, 2000.</small>	<small>Hartley and A. Zisserman. <i>Multiple View Geometry in Computer Vision</i>. Cambridge University Press, 2000.</small>	<small>Hartley and A. Zisserman. <i>Multiple View Geometry in Computer Vision</i>. Cambridge University Press, 2000.</small>	<small>Hartley and A. Zisserman. <i>Multiple View Geometry in Computer Vision</i>. Cambridge University Press, 2000.</small>	<small>Hartley and A. Zisserman. <i>Multiple View Geometry in Computer Vision</i>. Cambridge University Press, 2000.</small>
<small>The former is an high level I representation. A correct behaviour that is exhibited by an extended semantics for a database model</small>	<small>The former is an high level I representation. A correct behaviour that is exhibited by an extended semantics for a database model</small>	<small>The former is an high level I representation. A correct behaviour that is exhibited by an extended semantics for a database model</small>	<small>The former is an high level I representation. A correct behaviour that is exhibited by an extended semantics for a database model</small>	<small>The former is an high level I representation. A correct behaviour that is exhibited by an extended semantics for a database model</small>	<small>The former is an high level I representation. A correct behaviour that is exhibited by an extended semantics for a database model</small>	<small>The former is an high level I representation. A correct behaviour that is exhibited by an extended semantics for a database model</small>
<small>SSO uses a semantic data after concatenation and fusion.</small>	<small>SSO uses a semantic data after concatenation and fusion.</small>	<small>SSO uses a semantic data after concatenation and fusion.</small>	<small>SSO uses a semantic data after concatenation and fusion.</small>	<small>SSO uses a semantic data after concatenation and fusion.</small>	<small>SSO uses a semantic data after concatenation and fusion.</small>	<small>SSO uses a semantic data after concatenation and fusion.</small>

Fig. 4: Comparison of deblurred images by our method and other popular approaches on the images from BMVC_TEXT dataset [3]. (a) Blurred images. (b) Deblurring results using Pan [4]. (c) Deblurring results using Pan [5]. (d) Deblurring results using Xu [6]. (e) Deblurring results using Sun [2]. (f) Deblurring results using MS-CNN [7]. (g) Deblurring results using CycleGAN [1]. (h) Our results. It shows the characters in our results are much clearer.

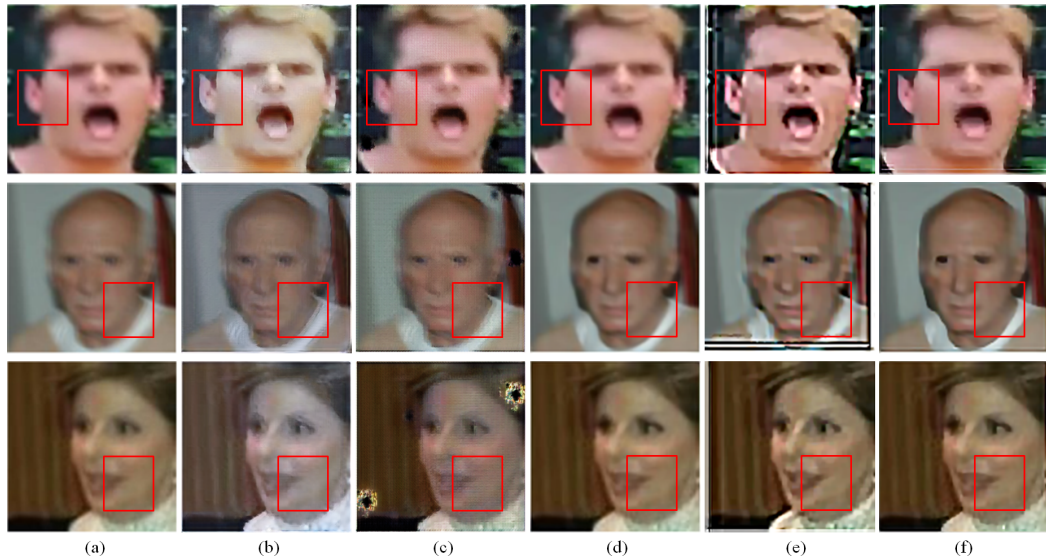


Fig. 5: Comparison of deblurred images by our method and other popular approaches on several images from face dataset [8]. (a) Blurred images. (b) Deblurring results using CycleGAN [1]. (c) Deblurring results using DiscoGAN [9]. (d) Deblurring results using MS-CNN [7]. (e) Deblurring results using Pan [5]. (f) Deblurring results by our method.